DAS-CGG17 GAS GENERATOR

Design description and parameters

DAS-CGG17-DS

Developed by		Checked by	
ПІБ Name	Дата та підпис Signature & Date	ПІБ Name	Дата та підпис Signature & Date
ПІБ Name	Дата та підпис Signature & Date	ПІБ Name	Дата та підпис Signature & Date

Approved by

Roman Marchan

ПІБ
Name

Дата та підпис
Signature & Date

TABLE OF CONTENTS

List of Abbreviations

AI - Acoustic Igniter

GG - Gas Generator

DD - Design Documentation

GOx - Gaseous Oxygen

LOx - Liquid Oxygen

L-PBF - Laser Powder Bed Fusion

Introduction

DAS-CGG17 gas generator developed by Dnipro Aerospace for Gilmour Aerospace, is intended for operation as a part of the 17.5 tf open cycle engine. GG runs on non-hypergolic propellants LOx/Jet A-1 in a fuel-rich cycle (see Figure 1).

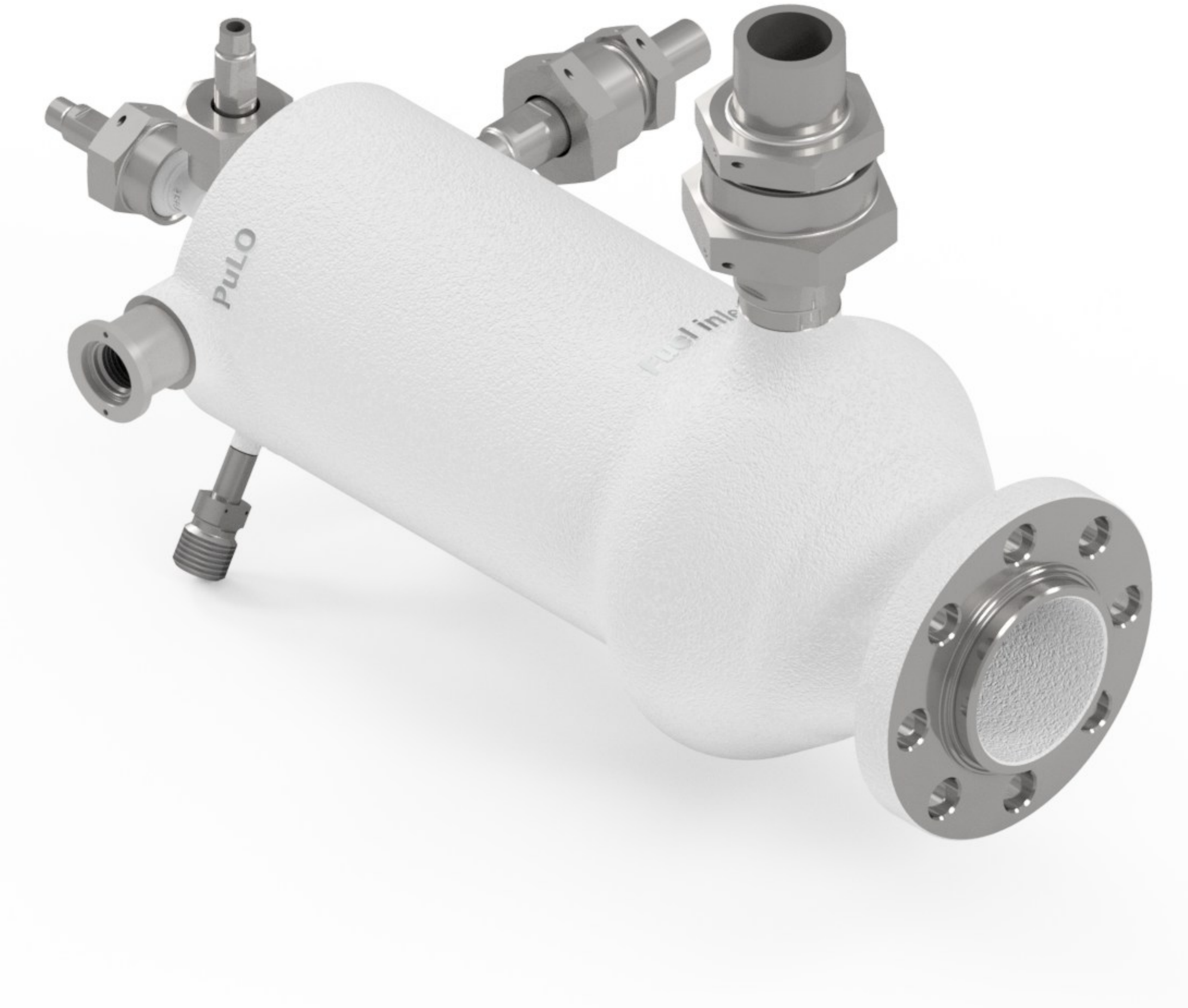

Figure 1 – DAS-CGG17 Gas Generator

1. Gas generator nominal parameters

Gas generator nominal parameters are presented in Table 1.1.

Table 1.1 – Gas generator nominal parameters

	Parameter	Units	Value
	Propellants Ox Fu		 Liquid Oxygen Jet A-1
	Total LOx pressure at GG inlet	bar	75±3
	Total kerosene pressure at GG inlet	bar	75±3
	Total gas pressure at GG outlet	bar	63.6
	Generator gas temperature	K	1048±26
	Mass mixture ratio in GG		0.36
	Total propellant flowrate through GG	kg/s	2.45
	Oxidizer flowrate through GG, including: LOx flowrate through injectors GOx flowrate through igniter Total flowrate	kg/s	 0.61 0.038 0.648
	Fuel flowrate through GG, including: Kerosene flowrate through injectors Kerosene flowrate through igniter Total flowrate	kg/s	 1.737 0.064 1.801
	LOx temperature at GG inlet	K	93^{+7}
	Kerosene temperature at GG inlet	K	299^{+11}_{-13}

2. Gas generator design description

The gas generator consists of a mixing head, a body and an acoustic igniter.

2.1 Mixing head

The mixing head consists of 6 centrifugal-centrifugal injectors evenly spaced around the circumference on the face plate. The external injector is for fuel, and the internal injector is for oxidizer (see Figure 2.1).

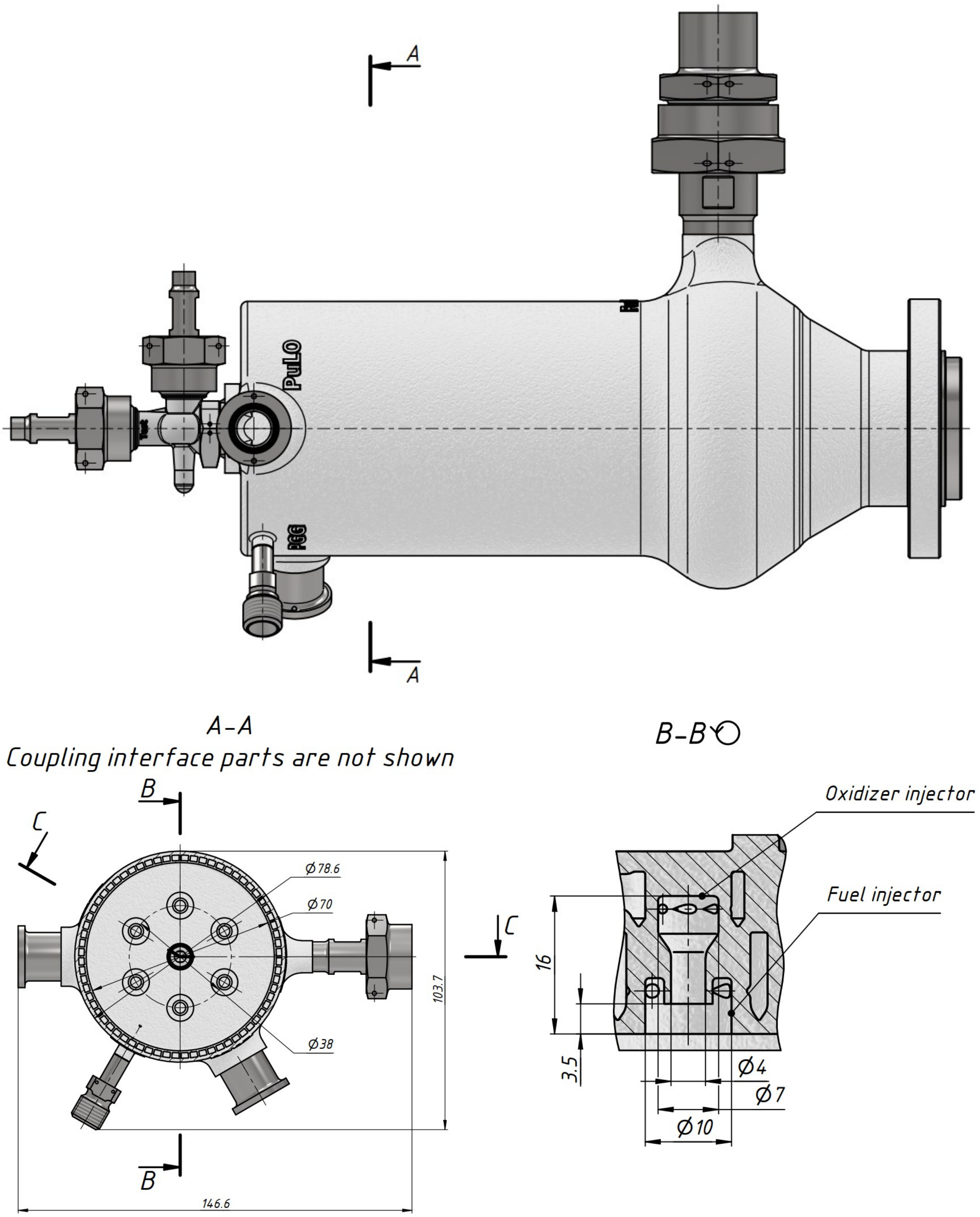

Figure 2.1 – Gas generator mixing head and its centrifugal-centrifugal injector

The oxidizer is supplied to the mixing head through a inlet pipe with a diameter of 8 mm. The fuel is supplied to the mixing head directly from the regenerative cooling line of the GG chamber body (see Figure 2.2).

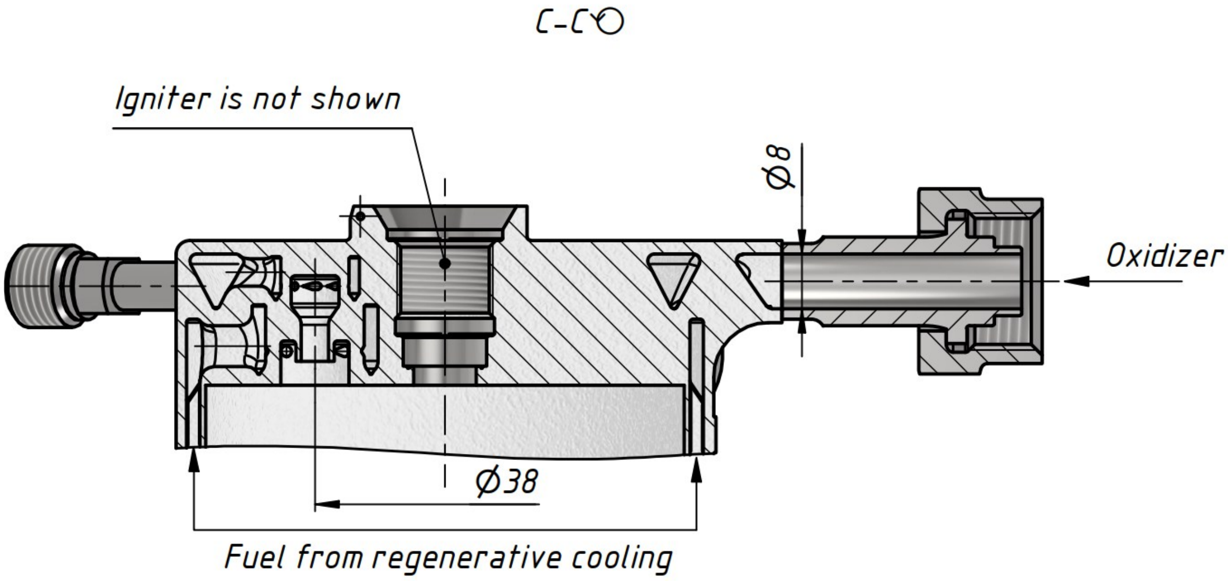

Figure 2.2 – Propellant supply to the GG mixing head

2.2 Gas generator body

The counter-flow fuel regenerative cooling helps to increase reliability of the body. The propellant is supplied through a ⌀18 mm branch pipe. The cooling scheme is shown in Figure 2.3.

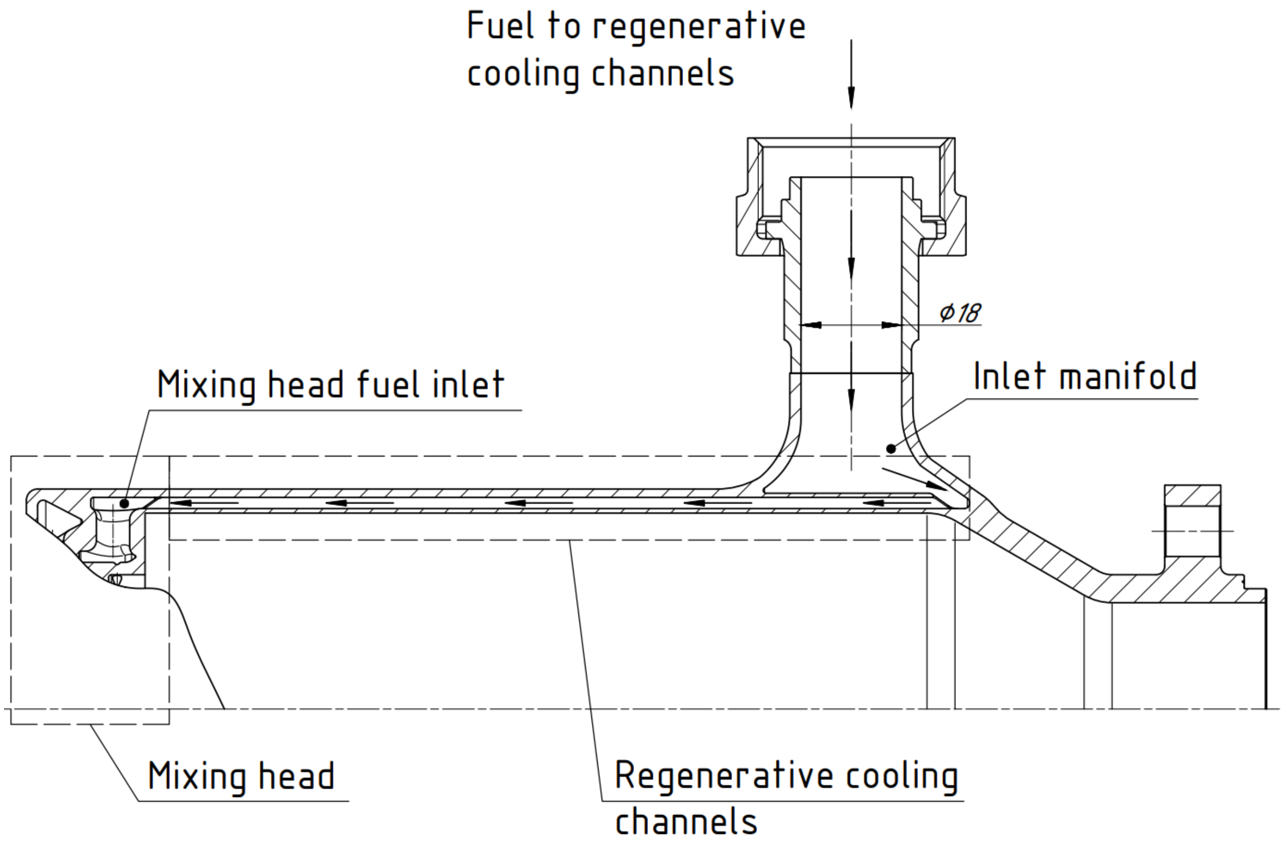

Figure 2.3 – Cooling scheme of the GG body (mixing head is not shown)

The geometry of the cooling channels was determined based on the results of the GG cooling analysis (see Table 2.1).

Table 2.1 – Geometry of the cooling channels based on the analysis results

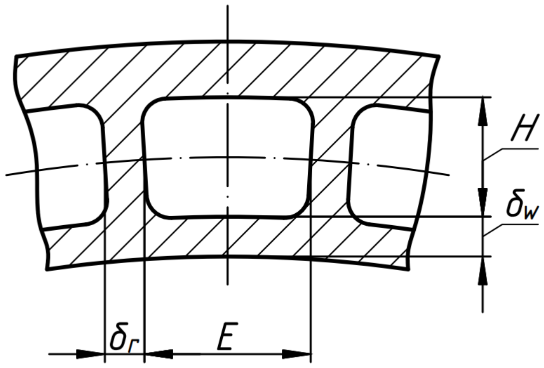

$\boldsymbol{H}$, mm	$\boldsymbol{\delta_w}$, mm	$\boldsymbol{E}$, mm	$\boldsymbol{\delta_r}$, mm	$\boldsymbol{N}$, pcs
2.0	0.8	2.70	0.7	68
N – number of cooling channels				

2.3 Acoustic igniter

The acoustic igniter is designed to ignite propellants at GG startup. The AI is manufactured from Haynes 230 powder using L-PBF additive technology. The obtained AI blank is machined to meet DD requirements for connecting interfaces. The general view is shown in Figure 2.4.

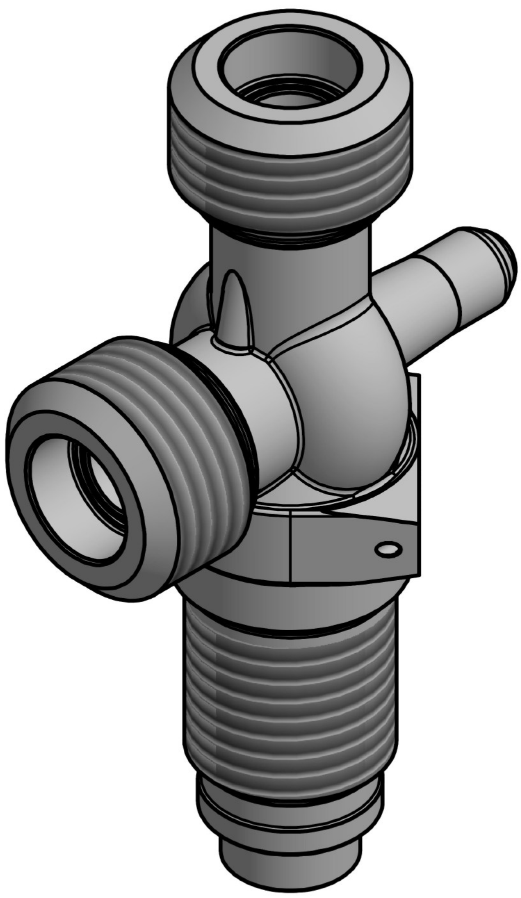

Figure 2.4 – Acoustic igniter general view

The AI uses gaseous oxygen as an oxidizer and Jet A-1 kerosene as a fuel.

Figure 2.5 shows AI flow passages. Oxidizer-rich gas is supplied to the ignition chamber (VII) through the sonic nozzle (I). The oxidizer sonic nozzle and the resonator (VI) jointly form a Hartmann-Sprenger generator.

Fuel flowrate is divided into two parts:

– ignition (III) (about 6% of the total fuel flowrate through AI);

– regenerative (IV) and film cooling (V) (about 94% of the total fuel flowrate through AI).

The film cooling consists of 6 tangential holes (IX) with a diameter of 0.9 mm.

The ignition channel (III) has a screw shape to dose fuel flowrate. The channel diameter (0.8 mm) was selected based on the required flowrate and printability.

Most of the fuel goes for regenerative cooling of ignition chamber (VII) and resonance tube (VI), as well as film cooling of the flame duct (VIII).

Figure 2.6 shows main geometry parameters of AI.

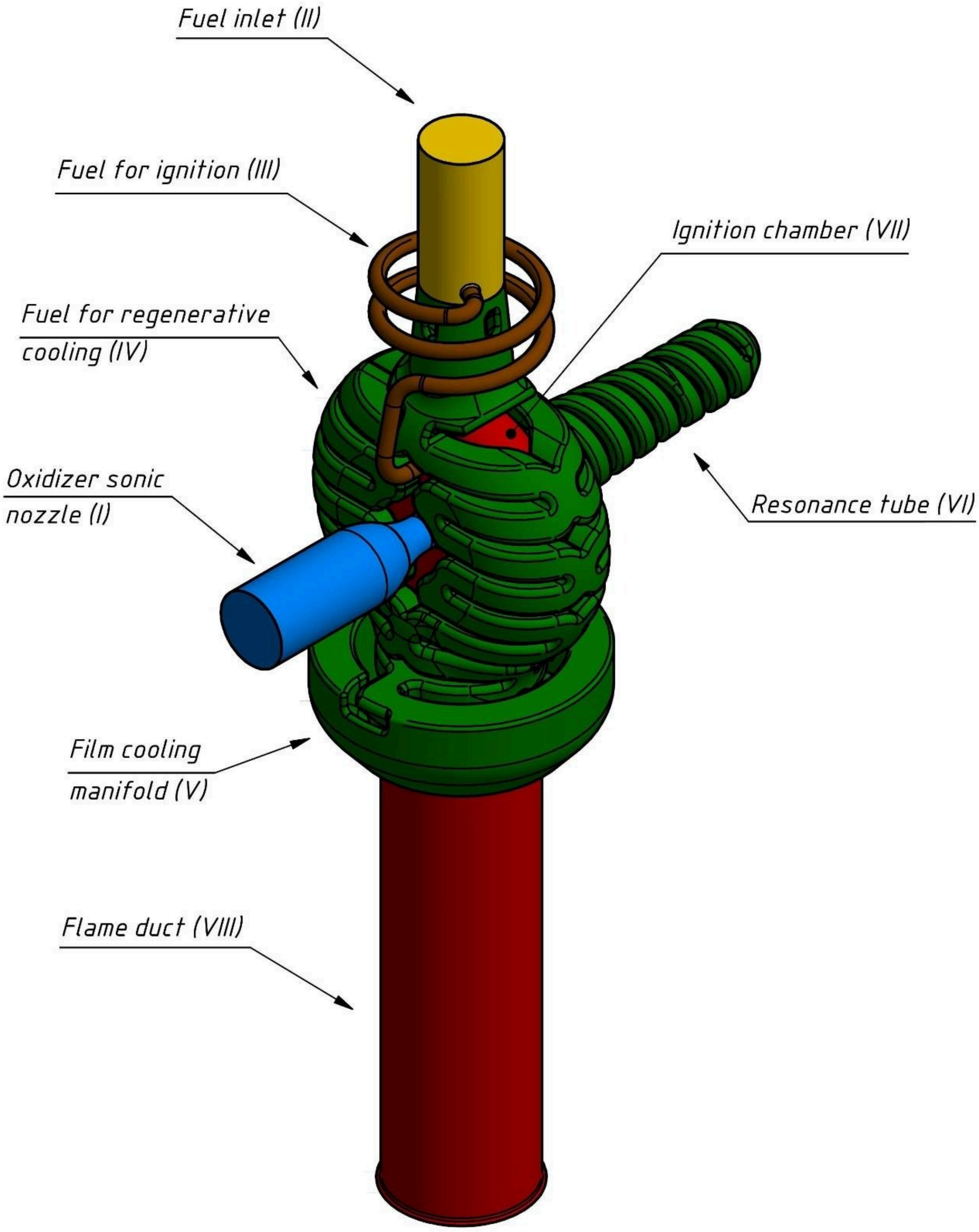

Figure 2.5 – Acoustic igniter flow passages

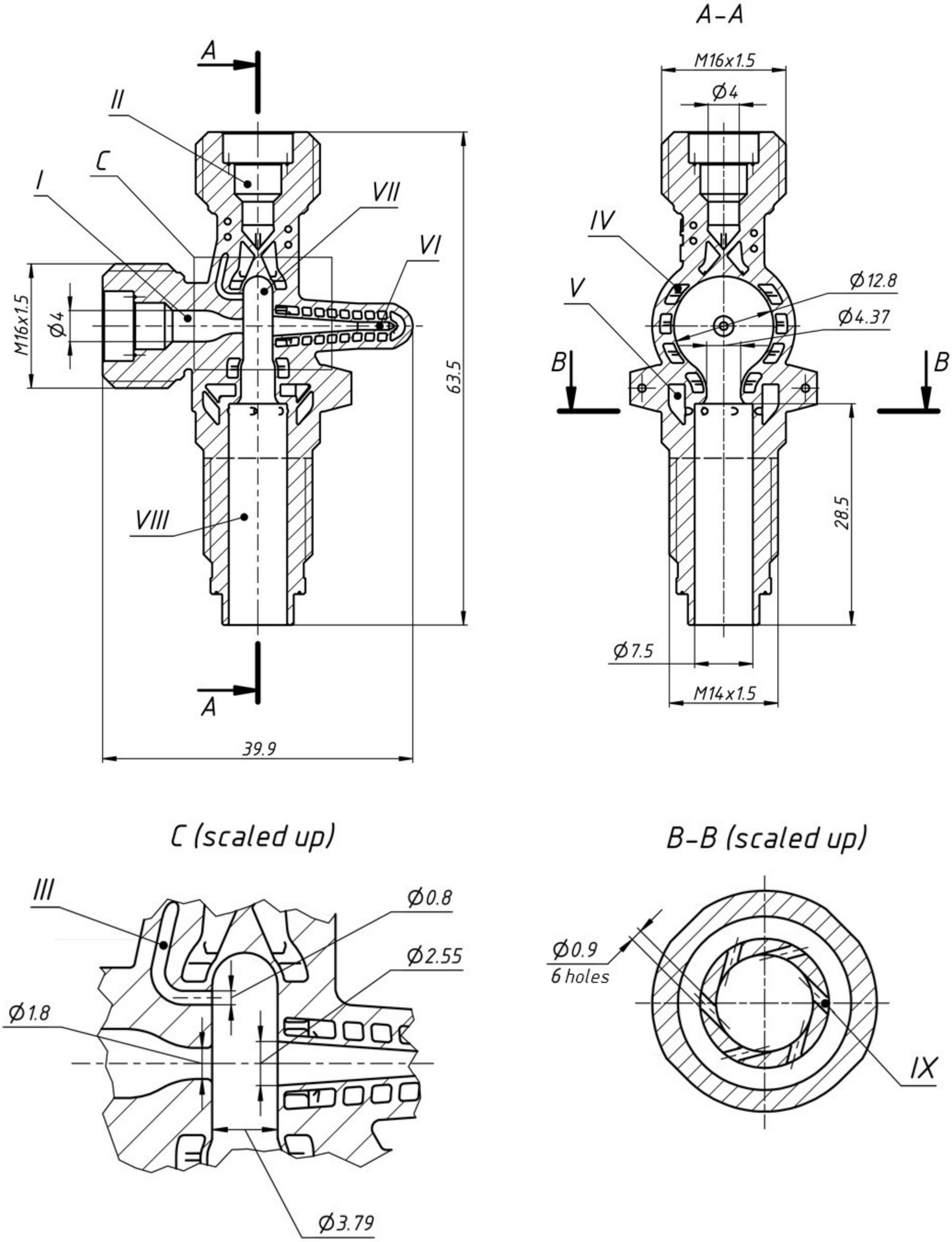

Figure 2.6 – Main geometry parameters of acoustic igniter

3. Gas generator simulation

To confirm design serviceability, the following was done: cooling analysis, hydraulic analysis, strength analysis, gas generator CFD simulation, acoustic analysis of the GG gas cavity in conjunction with the stator gas cavity.

3.1 Some results of GG hydraulic and cooling analyses

The GG body cooling analysis was performed in accordance with initial data given in Table 3.1.

Table 3.1 – Initial data for GG cooling analysis

Parameter	Value
Pressure in GG, bar	65
Mixture ratio	0.36
Total propellant flowrate	2.45
Fuel flowrate in the cooling channels, kg/s	1.737
Pressure losses in the cooling channels, bar	1

In the course of analysis, there was considered an operation mode with the greatest thermal load (taking into account the imperfection of the mixing system): a mode with a zone of increased mass mixture ratio at a distance of 70 mm from the mixing head. Under such conditions, the temperature of generator gas is 1110℃, which is slightly higher than the design value.

Analysis results are shown in Figures 3.1-3.4.

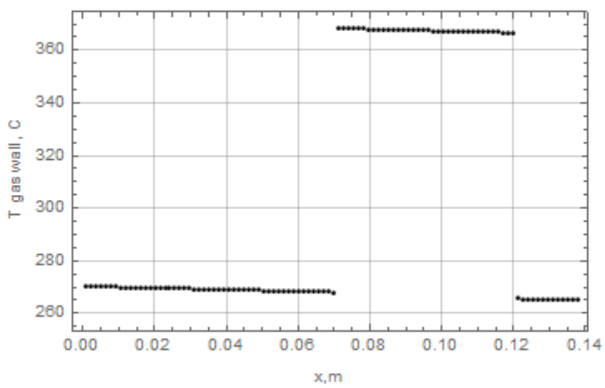

Figure 3.1 – Temperature of the wall on the combustion products side

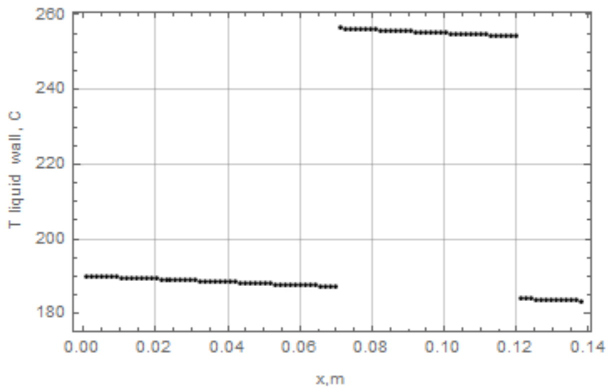

Figure 3.2 – Temperature of the wall on the coolant side

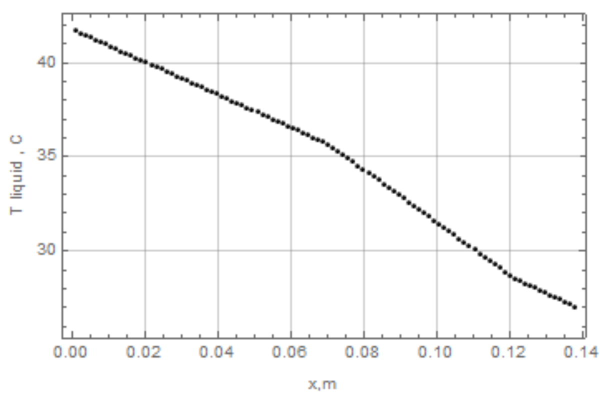

Figure 3.3 – Temperature of the kerosene in the cooling channels

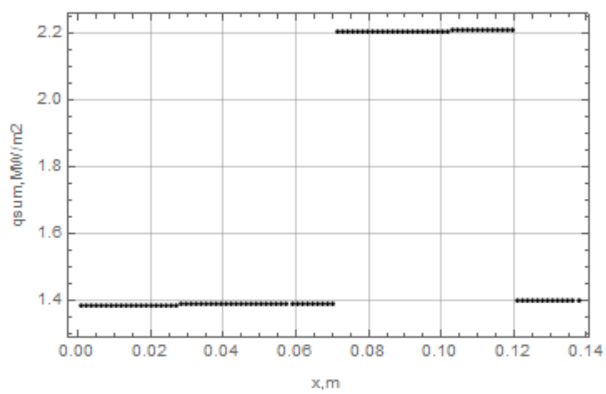

Figure 3.4 – Specific heat flux through the GG wall

Pressure losses in GG cooling channels were analyzed. Pressure differentials along the channels shall not exceed 10 bar.

3.2 Some results of CFD simulation

CFD simulation confirmed the results of hydraulic analysis. CFD simulation took into account the dependence of the surface roughness variation on the angle of the surface inclination during 3D printing.

3.2.1 Uniformity of propellants’ distribution in the mixing head

Mass flowrate

The deviation of the mass flowrate of one injector from the average value over the entire mixing head is no more than ~3.4%, which fully meets the conditions for high-quality mixing.

Based on the results of simulation, there were obtained the data on the distribution of flow velocity values in the mixing head (see Figure 3.5).

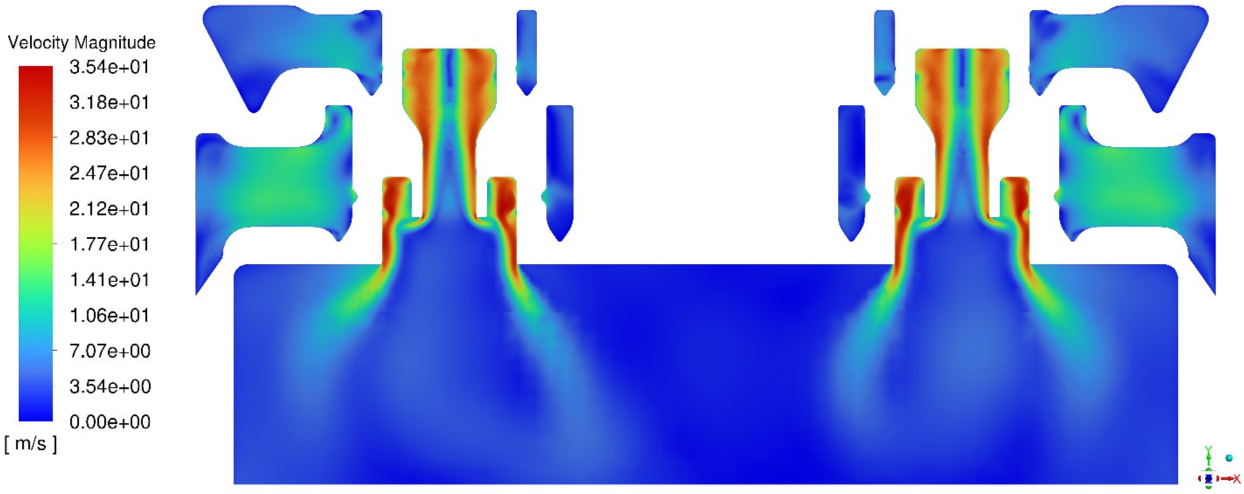

Figure 3.5 – Flow velocity distribution in the mixing head

Mixture ratio for each injector

Based on the results of CFD simulation, there were obtained propellant flowrates per 1 injector, the deviation from “ideal” – arithmetic-mean flowrate, as well as the mixture ratio for each injector (see Table 3.2).

Table 3.2 – Obtained flowrates distribution per 1 injector, propellant mixture ratio through 1 injector in the GG mixing head, as well as their percentage deviation

No.	m_f, kg/s	m_o, kg/s	k_m	δ_{mf},%	δ_{mo},%	δ_{mo},%
1	0.324	0.095	0.35	0.2%	-0.1%	-2.4%
2	0.322	0.096	0.36	-0.6%	0.9%	-1%
3	0.324	0.097	0.36	0.2%	2.3%	0%
4	0.319	0.096	0.36	-1.7%	1.5%	0.7%
5	0.322	0.094	0.35	-0.7%	-1.3%	-3.1%
6	0.324	0.092	0.34	0.01%	-3.4%	-5.8%

The numbers are assigned to injectors according to the scheme shown in Figure 3.6.

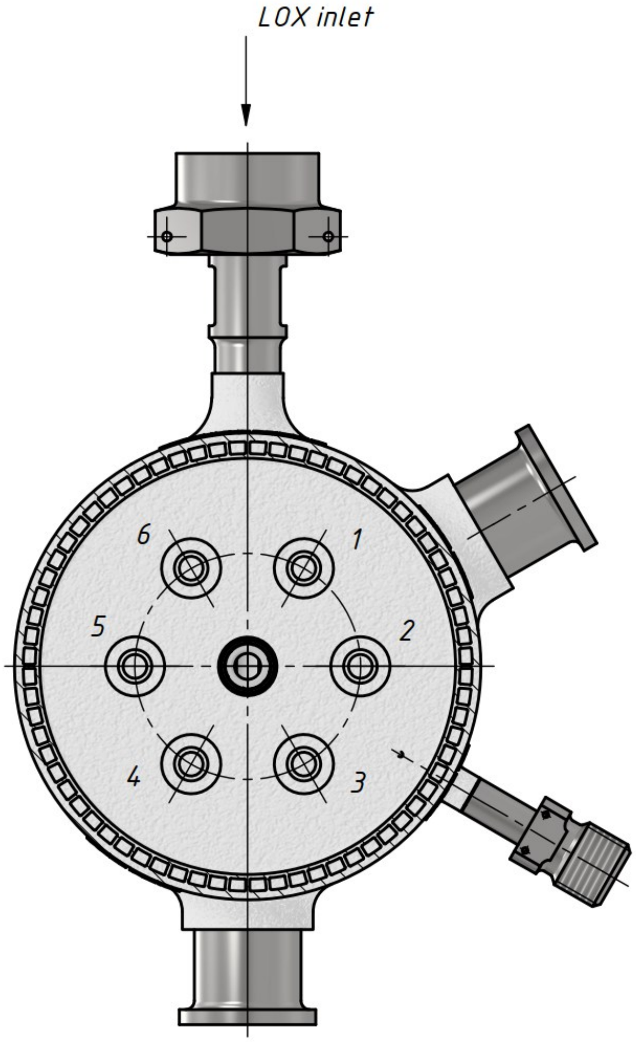

Figure 3.6 – Injectors numbering scheme

3.2.2 Pressure differentials along the lines

Based on the results of CFD simulation, there were determined the values of Ox and Fu static pressures that shall be provided at the GG propellants inlets (see Table 3.3).

Table 3.3 – Obtained values of static pressures at the inlets to GG Ox and Fu lines

P_o^{in}, bar	P_f^{in}, bar
10	10

Based on the results of CFD simulation, the following was concluded:

– GG design fully ensures necessary hydraulic characteristics in terms of considered pressure differentials, taking into account the dependence of the surface roughness in the lines on the geometry of the part;

– GG mixing head provides an acceptable spread in the uniformity of propellants distribution in the cross section of the GG chamber.

3.3 Gas generator strength analysis

There was performed an analysis of the GG structural strength, taking into account the characteristics of the temperature field distribution at the nominal operating mode and the corresponding properties of assembly units' materials. Based on the results of the strength analysis, design safety margins were determined (see Table 3.4, Figure 3.7).

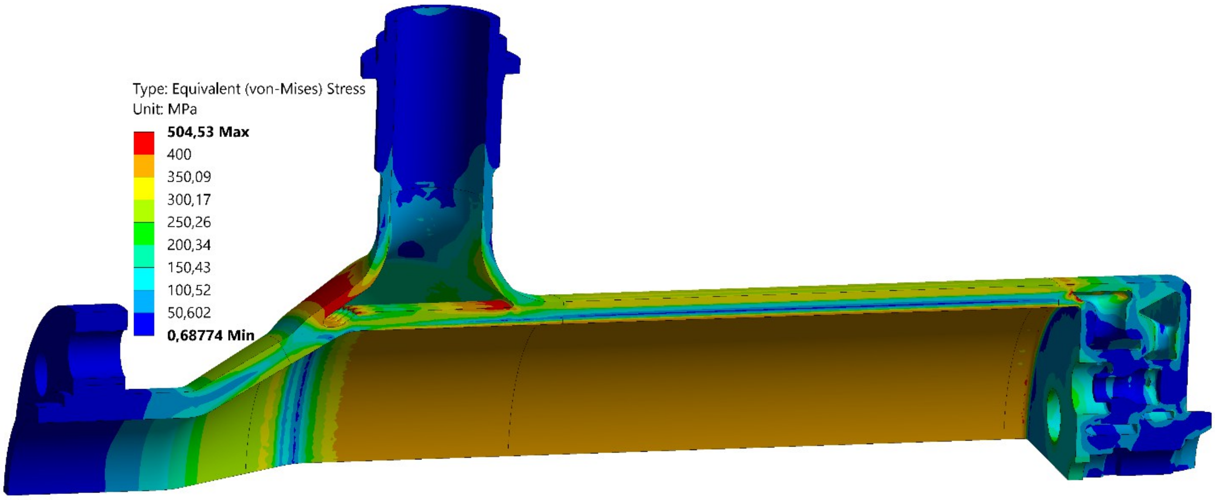

Figure 3.7 – Distribution of stresses in GG structure

Table 3.4 – Design safety margins of GG structure

Design stresses, MPa	Tensile strength safety margin (design value)	Yield strength safety margin (design value)
400	2.04	1.04

The analysis results showed that the GG design safety margins are sufficient. There are no relative plastic strains in the structure.

3.4 Acoustic igniter strength analysis

In order to confirm AI serviceability and corresponding safety margins in the course of its operation as a part of GG, there was performed strength analysis, taking into account the characteristics of the temperature field distribution in the structure. Based on the analysis results there was obtained the distribution of stresses arising in the AI structure (see Fig. 3.8). The obtained values of safety margins for tensile and yield strength are given in Table 3.5.

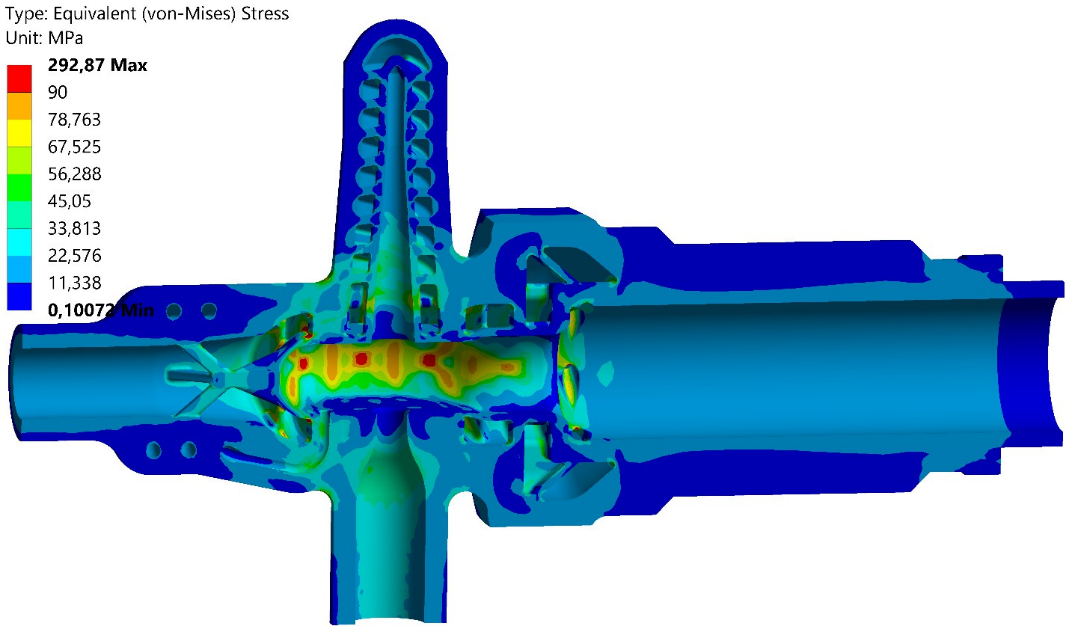

Figure 3.8 – Distribution of internal stresses based on the results of strength analysis

Table 3.5 – Design safety margins in the structure

Design stresses, MPa	Tensile strength safety margin (design value)	Yield strength safety margin (design value)
90	7.89	3.97

The analysis results showed that the AI design safety margins are sufficient. There are no relative plastic strains in the structure.

4. Recommended sequence for GG startup and shutdown

The recommended scheme to be used for GG startup and shutdown is shown in Figure 4.1. The list of symbols for measured parameters used in the scheme is given in Table 4.1.

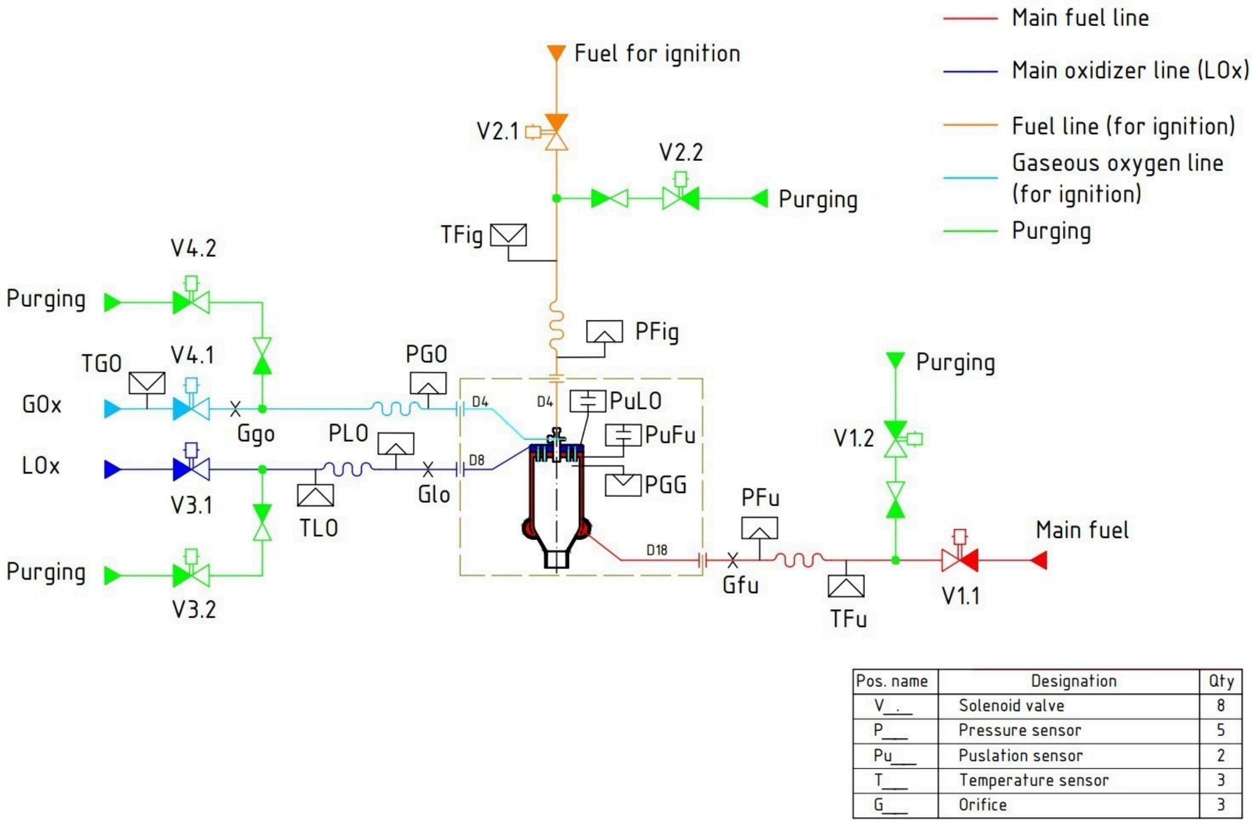

Figure 4.1 – Proposed flow diagram for the gas generator test

Table 4.1 – List of symbols for parameters recommended to be measured

Symbol	Purpose	Units
Main fuel line		
PFu	Fuel pressure at GG inlet	bar
Gfu	Orifice	-
PuFu	Fuel pressure pulsations before GG injectors	bar
TFu	Fuel temperature at GG inlet	K
Fuel line (for ignition)		
PFig	Fuel pressure at AI inlet	bar
TFig	Fuel temperature at AI inlet	K

The end of Table 4.1

Symbol	Purpose	Units
Gaseous oxygen line (for ignition)		
PGO	GOx pressure at AI inlet	bar
TGO	GOx temperature at AI inlet	K
Ggo	Orifice	-
Main oxidizer line (LOx)		
PLO	LOx pressure at GG inlet	bar
PuLO	LOx pressure pulsations before GG injectors	bar
TLO	LOx temperature at GG inlet	K
Glo	Orifice	-
GG cavity		
PGG	Pressure in GG fire cavity	bar

The recommended procedure of GG startup and shutdown according to the given scheme is provided below.

4.1 GG startup

GG startup sequence:

1) Start purging of LOx, GOx and main fuel supply lines: ↑ V1.2, V3.2, V4.2.
2) Stop purging of GOx supply line: ↓ V4.2.
Open GOx supply line: ↑V4.1
3) Open fuel supply line to AI: ↑V2.1
4) Stop purging of LOx supply line: ↓ V3.2
Open LOx supply line: ↑V3.1
5) Stop purging of main fuel supply line: ↓ V1.2
Open main fuel supply line: ↑V1.1

4.2 GG shutdown

GG shutdown sequence:

1) Start purging of LOx, main fuel and fuel for AI supply lines: ↑ V1.2, V2.2, V3.2.
2) Start purging of GOx supply line: ↑ V4.2
Close GOx and LOx supply lines: ↓V3.1, ↓V4.1
3) Close main fuel and fuel to AI supply lines: ↓V1.1, ↓V2.1
4) Stop purging of fuel supply lines: ↓V1.2, ↓V2.2.
5) Stop purging of oxidizer supply lines: ↓V3.2, ↓V4.2.

The recommended sequence of commands for opening and closing valves is given in Table 4.2.

Table 4.2 – Recommended sequence of commands during DAS-CGG17 GG tests

Step	Valve
0	Startup
1	↑ V1.2, V3.2, V4.2
2	↑V4.1
	↓ V4.2
3	↑V2.1
4	↑V3.1
	↓ V3.2
5	↑V1.1
	↓ V1.2
	Shutdown
6	↑ V1.2, V2.2, V3.2
7	↑ V4.2
	↓V3.1, ↓V4.1
8	↓V1.1, ↓V2.1
9	↓V1.2, ↓V2.2
10	↓V3.2, ↓V4.2